


Scattering of a Gaussian beam by an anisotropic-coated eccentric conducting circular cylinder

cambridge.org/mrf

Shi-Chun Mao¹ , Zhen-Sen Wu², Zhaohui Zhang¹, Jiansen Gao¹
and Lijuan Yang¹

Research Paper

Cite this article: Mao S-C, Wu Z-S, Zhang Z, Gao J, Yang L (2020). Scattering of a Gaussian beam by an anisotropic-coated eccentric conducting circular cylinder. *International Journal of Microwave and Wireless Technologies* **12**, 900–905. <https://doi.org/10.1017/S1759078720000434>

Received: 10 December 2019
Revised: 31 March 2020
Accepted: 1 April 2020
First published online: 27 April 2020

Keywords:

scattering; complex media; computational electromagnetics

Author for correspondence:

Shi-Chun Mao,
E-mail: mscgroup@163.com

¹Institute of Information Engineering, Suqian College, Suqian, Jiangsu 223800, China and ²School of Physics and Optoelectronic Engineering, Xidian University, Xi'an, Shaanxi 710071, China

Abstract

A solution to the problem of Gaussian beam scattering by a circular perfect electric conductor coated with eccentrically anisotropic media is presented. The incident Gaussian beam source is expanded as an approximate expression in the simple form with Taylor's series. The transmitted field in the anisotropically coated region is expressed as an infinite summation of Eigen plane waves with different polar angles. The unknown coefficients of the scattered fields are obtained with the aid of the boundary conditions. The addition theorem for cylindrical functions is applied to transfer from the local coordinates to the global ones. The infinite series can be truncated under the prerequisite of achieving the solution convergence. Only the case of transverse-electric polarization is discussed. The similar formulation of transverse-magnetic polarization can be obtained by adopting a similar method. Some numerical results are presented and discussed. The result is in agreement with that available as expected when the eccentric geometry comes to the concentric one.

Introduction

Solutions to the problem of electromagnetic scattering by cylindrical structures have been investigated theoretically in many papers [1, 2]. As regard to the scattering problem by anisotropic-coated conducting objects, an analytical solution of plane wave scattering by a circular perfect electromagnetic conductor cylinder coated with anisotropic media was presented in [3]. The incidence wave discussed in the aforementioned papers is limited to plane waves. With the development of laser sources and the tremendous expansion of their application, there has been a growing interest in the study of scattering by various particles illuminated by a Gaussian beam. For example, a two-dimensional beam is scattered by a cylinder buried below a slightly rough surface; scattering of a Gaussian beam from a row of cylinders with rectangular cross-section is studied in [4]; internal and near-surface electromagnetic fields for a uni-axial anisotropic cylinder illuminated with a Gaussian beam is discussed in [5].

The problem of scattering of a Gaussian beam by a circular perfect electric conductor (PEC) cylinder coated with eccentric anisotropic media is treated in this paper, which is an expansion of our previous works [6, 7]. There are a limited number of papers that treat the eccentric geometry (i.e. [8]). To the best of our knowledge, a circular PEC cylinder coated with an eccentric anisotropic shell illuminated by a Gaussian beam has not yet been discussed. Different from the expression of a 2D Gaussian beam in conventional analysis [9, 10], a simpler expression presented by Kozaki [11] is employed in this paper. In order to solve the boundary condition, the addition theorem for cylindrical functions is applied to transfer from the local coordinates to the global ones. Only the case of transverse-electric polarization is considered and the similar formulation of transverse-magnetic polarization can be obtained by adopting a similar method.

Formulation

As can be seen from Fig. 1, a cross-section of an infinitely long conducting circular cylinder coated with an eccentric anisotropic shell is shown. Three rectangular coordinate systems and one cylindrical coordinate system are defined, the z -axis which is common to these coordinate systems is not plotted. The global coordinate system (x, y) and the local coordinate system (x_c, y_c) are defined. The radii of cylinders are denoted by a and b , their axes are fixed at origins O_c and O , respectively. A Gaussian beam source which is located at $(x_1 = -r_0, y_1 = 0)$ is incident on the circular cylinder, making an angle θ_0 clockwise with respect to the negative x -axis.

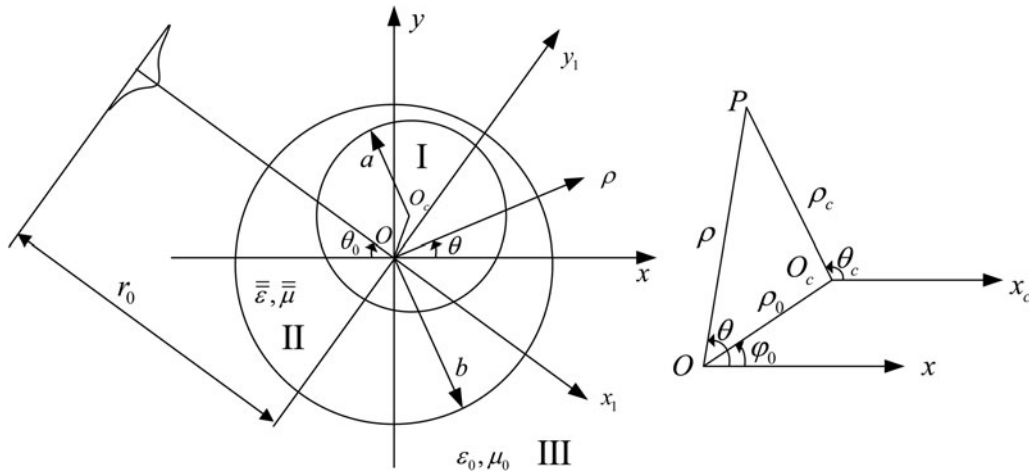


Fig. 1. Geometry of the problem.

Transmitted wave

In the expressions for the electromagnetic fields, the time dependence $\exp(j\omega t)$ is omitted throughout. Consider a homogeneous anisotropic medium characterized by the following permittivity and permeability tensors in the $X_cO_cY_c$ coordinate frame:

$$\bar{\bar{\epsilon}} = \begin{bmatrix} \epsilon_{xx} & \epsilon_{xy} & 0 \\ \epsilon_{yx} & \epsilon_{yy} & 0 \\ 0 & 0 & \epsilon_{zz} \end{bmatrix}, \bar{\bar{\mu}} = \begin{bmatrix} \mu_{xx} & \mu_{xy} & 0 \\ \mu_{yx} & \mu_{yy} & 0 \\ 0 & 0 & \mu_{zz} \end{bmatrix}. \tag{1}$$

The magnetic field in the annular region (part II) can be expressed in the local coordinates (x_c, y_c) as follows [12]

$$H_z(\rho_c, \theta_c) = \sum_{n=-\infty}^{\infty} j^{-n} \sum_{m=-\infty}^{\infty} [c_m^{(1)} F_{nm}^{(1)}(\rho_c, \theta_c) + c_m^{(2)} F_{nm}^{(2)}(\rho_c, \theta_c)], \tag{2}$$

where

$$F_{nm}^{(1)}(\rho_c, \theta_c) = \int_0^{2\pi} J_n(k(\xi)\rho_c) e^{j[n\theta_c + (m-n)\xi]} d\xi, \tag{3}$$

$$F_{nm}^{(2)}(\rho_c, \theta_c) = \int_0^{2\pi} Y_n(k(\xi)\rho_c) e^{j[n\theta_c + (m-n)\xi]} d\xi, \tag{4}$$

where $c_m^{(1)}$ and $c_m^{(2)}$ are unknown coefficients, $J_n[k(\xi)\rho_c]$ and $Y_n[k(\xi)\rho_c]$ are the Bessel functions of the first and second kind, respectively.

The tangential component of the electric field in the annular region (part II) can be expressed as

$$j\omega\gamma E_\theta^c = - \left[\epsilon_{\rho_c, \rho_c}(\theta_c) \frac{\partial H_z^c}{\partial \rho_c} + \epsilon_{\theta_c, \rho_c}(\theta_c) \frac{1}{\rho_c} \frac{\partial H_z^c}{\partial \theta_c} \right], \tag{5}$$

where

$$\begin{aligned} \epsilon_{\rho_c, \rho_c}(\theta_c) &= \epsilon_+ + \epsilon_- \cos 2\theta_c + \sigma_+ \sin 2\theta_c, \\ \epsilon_{\theta_c, \rho_c}(\theta_c) &= -\sigma_- + \sigma_+ \cos 2\theta_c - \epsilon_- \sin 2\theta_c. \end{aligned} \tag{6}$$

$$\begin{aligned} \epsilon_\pm &= \frac{1}{2}(\epsilon_{xx} \pm \epsilon_{yy}), \\ \sigma_\pm &= \frac{1}{2}(\epsilon_{xy} \pm \epsilon_{yx}). \end{aligned} \tag{7}$$

Incident and scattered waves

Consider the case where a beam source (e.g. a horn antenna) is located at $x_1 = -r_0$ as illustrated in Fig. 1. The z -component of the magnetic field of the incident Gaussian beam source is expressed in the global coordinate system (x, y) as follows [11]

$$H_z^{inc}(x_1 = -r_0, y_1) = e^{-\beta^2 y_1^2}, \tag{8}$$

where

$$\beta^2 = a_0^2 + j b_0^2, \tag{9}$$

where $1/|\beta|$ corresponds to the beamwidth of the incident wave. The parameters a_0, b_0 are determined from the distributions of amplitude and phase.

The incidence beam can be expressed as following [11]

$$H_z^{inc}(x_1, y_1) = \frac{1}{2\sqrt{\pi}\beta} \int_{-\infty}^{\infty} e^{(-\alpha^2/4\beta^2 - j(x_1+r_0)\sqrt{k_0^2-\alpha^2} - j\alpha y_1)} d\alpha. \tag{10}$$

For polar coordinates (ρ, θ) , equation (10) can be expressed as:

$$H_z^{inc}(\rho, \theta) = \sum_{n=-\infty}^{\infty} j^{-n} e^{jn\theta} J_n(k_0\rho) A_n^h, \tag{11}$$

where

$$A_n^h \cong A_{n1}^h = \frac{e^{-jk_0 r_0}}{\sqrt{1-jZ_0}} e^{-((n/k_0)\beta)^2/(1-jZ_0)}, \tag{12}$$

where $Z_0 = (2\beta^2 r_0)/k$. This expression is valid for $|(\beta\lambda)^2| < 0.3$ and $b/\lambda < 3.0$. For $(b/\lambda) \cong (3 \sim 5)$, an improved representation must be

used:

$$A_n^h \cong A_{n2}^h = A_{n1}^h \left[1 - 2 \left(\frac{\beta}{k_0 \sqrt{1 - jZ_0}} \right)^4 n^2 + \frac{4}{3} \left(\frac{\beta}{k_0 \sqrt{1 - jZ_0}} \right)^6 n^4 + \dots \right]. \tag{13}$$

Meanwhile, the scattered magnetic field in the free space region (part III) is expressed as

$$H_z^s(\rho, \theta) = \sum_{n=-\infty}^{\infty} B_n j^{-n} H_n^{(2)}(k\rho) e^{jn\theta}, \tag{14}$$

where B_n are unknown coefficients.

The tangential component of the electric field can be written in the global coordinate system (x, y) as follows:

$$E_\theta^{inc}(\rho, \theta) = j \sqrt{\frac{\mu_0}{\epsilon_0}} \sum_{n=-\infty}^{\infty} A_n j^{-n} J'_n(k\rho) e^{jn(\theta+\theta_0)}, \quad (\rho \geq b), \tag{15}$$

$$E_\theta^s(\rho, \theta) = j \sqrt{\frac{\mu_0}{\epsilon_0}} \sum_{n=-\infty}^{\infty} B_n j^{-n} H_n^{(2)'}(k\rho) e^{jn\theta}, \quad (\rho \geq b). \tag{16}$$

Boundary conditions

(1) Boundary Conditions on the Core Surface:

Assume the surface of the conducting circular cylinder is represented by $\rho_c = a$, the electric field vanishes on the surface of the conducting circular cylinder, the boundary condition can be written as

$$E_\theta^c(\rho_c, \theta_c) = 0, \quad (\rho_c = a). \tag{17}$$

i.e.

$$\sum_{m=-\infty}^{\infty} [c_m^{(1)} E_{nm}^{(11)}(a) + c_m^{(2)} E_{nm}^{(12)}(a)] = 0, \tag{18}$$

where

$$E_{nm}^{(11)}(a) = -j \sqrt{\frac{\epsilon_0}{\mu_0}} \int_0^{2\pi} \frac{k(\xi)}{\omega\gamma} e^{j(m-n)\xi} \times \left[j\epsilon_{\rho_c, \rho_c}(\xi) J'_n(k(\xi)a) - \frac{n\epsilon_{\theta_c, \rho_c}(\xi + \pi/2)}{k(\xi)a} J_n(k(\xi)a) \right] d\xi, \tag{19}$$

$$E_{nm}^{(12)}(a) = -j \sqrt{\frac{\epsilon_0}{\mu_0}} \int_0^{2\pi} \frac{k(\xi)}{\omega\gamma} e^{j(m-n)\xi} \times \left[j\epsilon_{\rho_c, \rho_c}(\xi) Y'_n(k(\xi)a) - \frac{n\epsilon_{\theta_c, \rho_c}(\xi + \pi/2)}{k(\xi)a} Y_n(k(\xi)a) \right] d\xi. \tag{20}$$

(1) Boundary Conditions on the External Surface: The tangential components of the electric and magnetic fields are continuous on the surface of anisotropic-free space, the boundary conditions can be expressed as

$$H_z^c = H_z^{inc} + H_z^s, \quad (\rho = b), \tag{21}$$

$$E_\theta^c = E_\theta^{inc} + E_\theta^s, \quad (\rho = b). \tag{22}$$

This requires that the fields be expressed in terms of the $X_c O_c Y_c$ coordinate frame be translated to the XOY coordinate frame using the addition theorem for cylindrical functions, i.e. [13]:

$$J_n(k(\xi)\rho_c) e^{jn\theta_c} = \sum_{m=-\infty}^{\infty} J_m(k(\xi)\rho) J_{m-n}(k(\xi)\rho_0) e^{j[m\theta - (m-n)\varphi_0]} \quad (\rho > \rho_0), \tag{23}$$

$$Y_n(k(\xi)\rho_c) e^{jn\theta_c} = \sum_{m=-\infty}^{\infty} Y_m(k(\xi)\rho) J_{m-n}(k(\xi)\rho_0) e^{j[m\theta - (m-n)\varphi_0]} \quad (\rho > \rho_0). \tag{24}$$

The magnetic field in the annular region (part II in Fig. 1) can be expressed in the global coordinates (x, y) as follows

$$H_z^c(\rho, \theta) = \sum_{n=-\infty}^{\infty} j^{-n} \sum_{m=-\infty}^{\infty} [c_m^{(1)} F_{nm}^{(1)}(\rho, \theta) + c_m^{(2)} F_{nm}^{(2)}(\rho, \theta)], \tag{25}$$

where

$$F_{nm}^{(1)}(\rho, \theta) = \sum_{i=-\infty}^{\infty} e^{j[i\theta - (i-n)\varphi_0]} \int_0^{2\pi} J_i(k(\xi)\rho) J_{i-n}(k(\xi)\rho_0) e^{j(m-n)\xi} d\xi, \tag{26}$$

$$F_{nm}^{(2)}(\rho, \theta) = \sum_{i=-\infty}^{\infty} e^{j[i\theta - (i-n)\varphi_0]} \int_0^{2\pi} Y_i(k(\xi)\rho) J_{i-n}(k(\xi)\rho_0) e^{j(m-n)\xi} d\xi. \tag{27}$$

Applying the boundary conditions (21) and (22), two equations can be obtained as

$$\sum_{n=-\infty}^{\infty} j^{-n} e^{-j(l-n)\varphi_0} \sum_{m=-\infty}^{\infty} [c_m^{(1)} F_{nm}^{(21)}(b) + c_m^{(2)} F_{nm}^{(22)}(b)] \tag{28}$$

$$= A_l J_l(kb) e^{jl\theta_0} + B_l H_l^{(2)}(kb),$$

$$\sum_{n=-\infty}^{\infty} j^{-n} e^{-j(l-n)\varphi_0} \sum_{m=-\infty}^{\infty} [c_m^{(1)} E_{nm}^{(21)}(b) + c_m^{(2)} E_{nm}^{(22)}(b)] \tag{29}$$

$$= A_l J'_l(kb) e^{jl\theta_0} + B_l H_l^{(2)'}(kb),$$

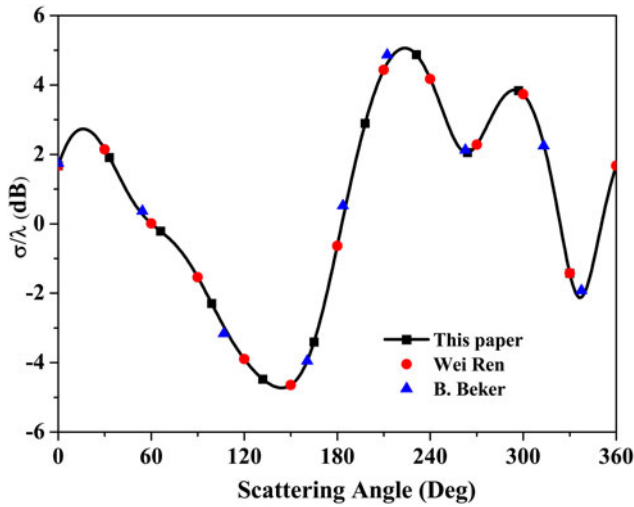


Fig. 2. *H*-polarization, bistatic radar cross-sections RCS dB, $\epsilon_{xx} = 1.5\epsilon_0$, $\epsilon_{yy} = 2.5\epsilon_0$, $\epsilon_{xy} = -\epsilon_{yx} = 3\epsilon_0$, $\mu_{zz} = 1.5\mu_0$, $(r_0/\lambda) = 3.0$, $ka = 1$, $kb = 2$, $\rho_0 = 0$, $\varphi_0 = 0^\circ$, $\theta_0 = 0^\circ$.

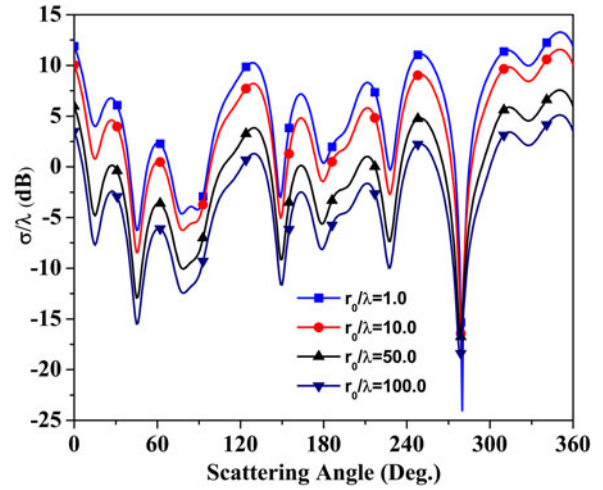


Fig. 4. *H*-polarization, bistatic radar cross-sections RCS dB, $\epsilon_{xx} = 2\epsilon_0$, $\epsilon_{yy} = \epsilon_0$, $\epsilon_{xy} = -\epsilon_{yx} = \epsilon_0$, $\mu_{zz} = 2\mu_0$, $ka = \pi$, $kb = 2\pi$, $\varphi_0 = 0^\circ$, $\theta_0 = 0^\circ$, $a_0\lambda = 0.2$, $b_0\lambda = 0.5$, $(\rho_0/a) = 0.2$.

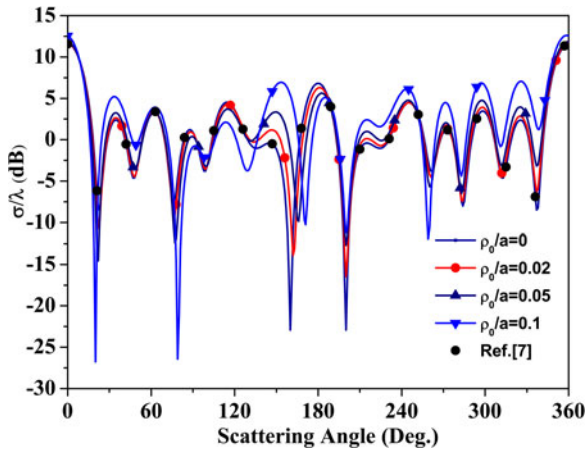


Fig. 3. *H*-polarization, bistatic radar cross-sections RCS dB, $\epsilon_{xx} = 4\epsilon_0$, $\epsilon_{yy} = \epsilon_0$, $\epsilon_{xy} = \epsilon_{yx} = 0$, $\mu_{zz} = 2\mu_0$, $ka = \pi$, $kb = 2\pi$, $\varphi_0 = 0^\circ$, $\theta_0 = 0^\circ$, $(r_0/\lambda) = 30.0$, $a_0\lambda = 0.2$, $b_0\lambda = 0.4$.

where

$$F_{nm}^{(21)}(b) = \int_0^{2\pi} J_l(k(\xi)b) J_{l-n}(k(\xi)\rho_0) e^{j(m-n)\xi} d\xi, \quad (30)$$

$$F_{nm}^{(22)}(b) = \int_0^{2\pi} Y_l(k(\xi)b) J_{l-n}(k(\xi)\rho_0) e^{j(m-n)\xi} d\xi, \quad (31)$$

$$E_{nm}^{(21)}(b) = -j\sqrt{\frac{\epsilon_0}{\mu_0}} \int_0^{2\pi} \frac{k(\xi)}{\omega\gamma} J_{l-n}(k(\xi)\rho_0) e^{j(m-n)\xi} \times \left[j\epsilon_{\rho\rho}(\xi) J_l'(k(\xi)b) - \frac{l\epsilon_{\theta\rho}(\xi + \pi/2)}{k(\xi)b} J_l(k(\xi)b) \right] d\xi, \quad (32)$$

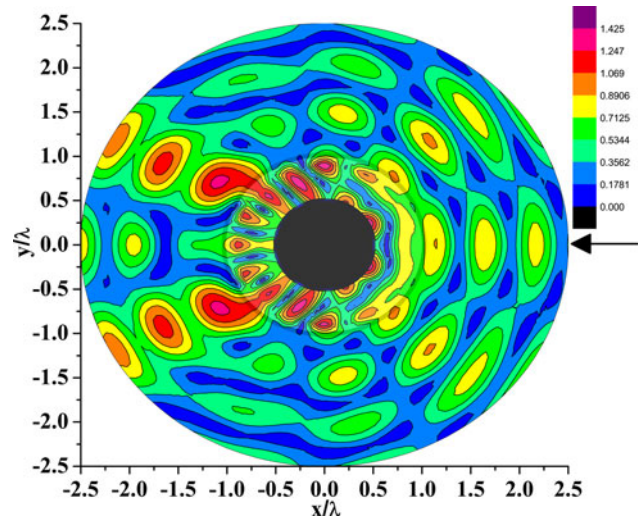


Fig. 5. The absolute value of the total magnetic field $|H_z|$ near the scatterer. $\epsilon_{xx} = 2\epsilon_0$, $\epsilon_{yy} = \epsilon_0$, $\epsilon_{xy} = \epsilon_{yx} = 0$, $\mu_{zz} = 2\mu_0$, $ka = \pi$, $kb = 2\pi$, $\theta_0 = 180^\circ$, $(r_0/\lambda) = 30.0$, $a_0\lambda = 0$, $b_0\lambda = 0$, $(\rho_0/a) = 0$, $\varphi_0 = 0^\circ$.

$$E_{nm}^{(22)}(b) = -j\sqrt{\frac{\epsilon_0}{\mu_0}} \int_0^{2\pi} \frac{k(\xi)}{\omega\gamma} J_{l-n}(k(\xi)\rho_0) e^{j(m-n)\xi} \times \left[j\epsilon_{\rho\rho}(\xi) Y_l'(k(\xi)b) - \frac{l\epsilon_{\theta\rho}(\xi + \pi/2)}{k(\xi)b} Y_l(k(\xi)b) \right] d\xi. \quad (33)$$

In order to obtain numerical results, the infinite series need to be truncated under the prerequisite of achieving the solution convergence. Truncating these equations for $-N \leq n \leq N$ and $-N \leq m \leq N$, they can be formed in vectors and matrices, the unknown coefficients can be obtained from these equations finally, and the electromagnetic field can be calculated while the radar cross-

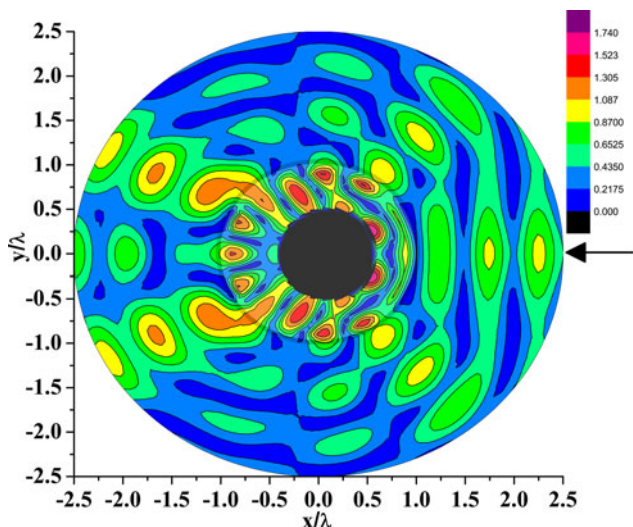


Fig. 6. The absolute value of the total magnetic field $|H_z|$ near the scatterer. $\epsilon_{xx} = 2\epsilon_0$, $\epsilon_{yy} = \epsilon_0$, $\epsilon_{xy} = \epsilon_{yx} = 0$, $\mu_{zz} = 2\mu_0$, $ka = \pi$, $kb = 2\pi$, $\theta_0 = 180^\circ$, $(r_0/\lambda) = 30.0$, $a_0\lambda = 0.3$, $b_0\lambda = 0.4$, $(\rho_0/a) = 0.2$, $\varphi_0 = 0^\circ$.

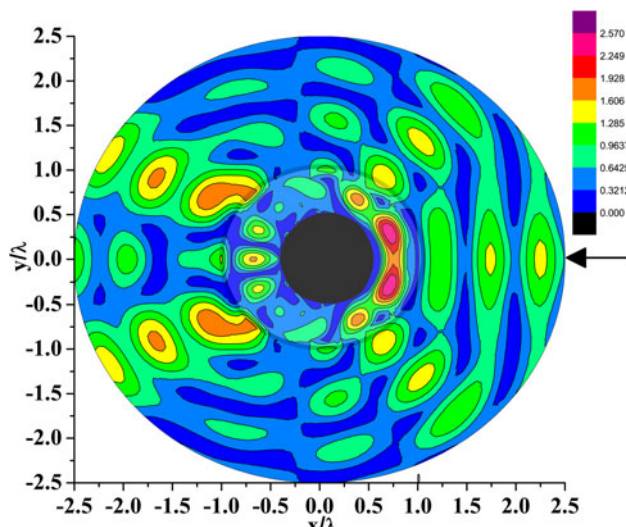


Fig. 8. The absolute value of the total electric field $|E_\theta|$ near the scatterer. $\epsilon_{xx} = 2\epsilon_0$, $\epsilon_{yy} = \epsilon_0$, $\epsilon_{xy} = \epsilon_{yx} = 0$, $\mu_{zz} = 2\mu_0$, $ka = \pi$, $kb = 2\pi$, $\theta_0 = 180^\circ$, $(r_0/\lambda) = 3.0$, $a_0\lambda = 0.3$, $b_0\lambda = 0.4$, $(\rho_0/a) = 0.2$, $\varphi_0 = 0^\circ$.

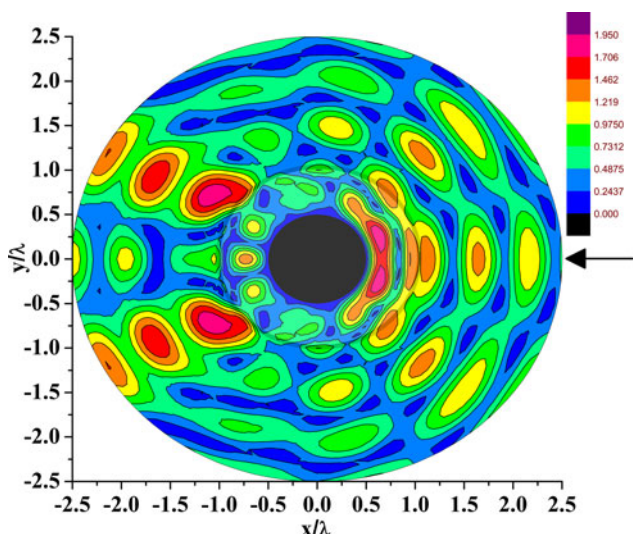


Fig. 7. The absolute value of the total electric field $|E_\theta|$ near the scatterer. $\epsilon_{xx} = 2\epsilon_0$, $\epsilon_{yy} = \epsilon_0$, $\epsilon_{xy} = \epsilon_{yx} = 0$, $\mu_{zz} = 2\mu_0$, $ka = \pi$, $kb = 2\pi$, $\theta_0 = 180^\circ$, $(r_0/\lambda) = 3.0$, $a_0\lambda = 0$, $b_0\lambda = 0$, $(\rho_0/a) = 0$, $\varphi_0 = 0^\circ$.

section per unit length (RCS) can be written as:

$$\frac{\sigma}{\lambda}(\theta, \theta^{inc}) = \frac{2}{\pi} \left| \sum_{n=-\infty}^{+\infty} B_n e^{jn\theta} \right|^2. \tag{34}$$

Numerical results

In this section, the variations of RCS versus the eccentricity, the distance between the laser and the scatterer are depicted; the total field distribution around the scatterer is listed and discussed. In order to check the validity and accuracy of the proposed method and associated code, the angular distributions of RCS are shown in Figs 2 and 3. A conducting circular cylinder covered with an eccentric anisotropic shell approaches a concentrically

circular geometry in both cases. For the plane wave incidence case [12, 14] in Fig. 2, both a_0 and b_0 are set to be zero, while $r_0/\lambda = 3.0$, $ka = 1$, $kb = 2$, $\rho_0 = 0$, $\varphi_0 = 0^\circ$, $\theta_0 = 0^\circ$, $N = 12$. The elements in the permittivity tensor and the permeability tensor are: $\epsilon_{xx} = 1.5\epsilon_0$, $\epsilon_{yy} = 2.5\epsilon_0$, $\epsilon_{xy} = -\epsilon_{yx} = 3\epsilon_0$, $\mu_{zz} = 1.5\mu_0$. For the Gaussian beam incidence case in Fig. 3, the parameters are: $\epsilon_{xx} = 4\epsilon_0$, $\epsilon_{yy} = \epsilon_0$, $\epsilon_{xy} = \epsilon_{yx} = 0$, $\mu_{zz} = 2\mu_0$, $ka = \pi$, $kb = 2\pi$, $\rho_0 = 0$, $\varphi_0 = 0^\circ$, $\theta_0 = 0^\circ$, $r_0/\lambda = 30.0$, $a_0\lambda = 0.2$, $b_0\lambda = 0.4$, $N = 15$. The results come into excellent agreement with those from [6] for the concentric geometry case.

Figure 3 also gives the effects of the different distance between the conducting and the anisotropic cylinder shell, i.e. the influence of the eccentricity on the values of RCS. This example consists of media with \hat{x} and \hat{y} principal axes. Compared with the concentric case, the graphics of non-concentric radar scattering are no longer symmetrically distributed with the scattering angles. The maximum values of RCS increase with the values of core eccentricity.

Figure 4 shows the effects of the distance between the laser source and the circular cylinder. The parameters are: $\epsilon_{xx} = 2\epsilon_0$, $\epsilon_{yy} = \epsilon_0$, $\epsilon_{xy} = -\epsilon_{yx} = \epsilon_0$, $\mu_{zz} = 2\mu_0$, $ka = \pi$, $kb = 2\pi$, $\varphi_0 = 0^\circ$, $\theta_0 = 0^\circ$, $a_0\lambda = 0.2$, $b_0\lambda = 0.5$, $\rho_0/a = 0.2$, $N = 15$. The whole RCS decline with the increase of the source distance.

Figures 5–8 show the absolute value of the total field near the scatterer, the arrow indicates the direction of the incident wave. Figures 5 and 6 represent two cases of magnetic field. It can be seen that there is a similar figure in concentric and non-concentric cases. The PEC acts as an impedance dielectric medium for magnetic field, it carries the Gaussian beam from the right to the anisotropic medium. Figures 7 and 8 represent two cases of electric field. The role of PEC in magnetic field and electric field is different. The tangential components of electric field vanish in PEC. The PEC acts like a mirror, blocking the transmission of electric field.

Conclusion

In conclusion, a solution to the two-dimensional scattering of a Gaussian beam by an anisotropic-coated eccentric conducting circular cylinder has been formulated in this paper, an approximate

expression presented by Kozaki of a Gaussian beam is utilized to treat the scattering problem. The addition theorem for cylindrical functions is applied to transfer from the local coordinates to the global ones. The result is in agreement with that available as expected when the eccentric geometry comes to the concentric one. The variations of RCS versus the eccentricity, the distance between the laser and the scatterer, the total field distribution around the scatterer are depicted and discussed in the numerical results section. It is demonstrated that it is possible to achieve large RCS values by choosing properly the eccentricity and the thickness of the shell.

Acknowledgements. This work was supported by the National Natural Science Foundation of China (Grant No. 61571355).

References

- Mizrahi E and Melamed T (2018) Plane wave scattering by a moving PEC circular cylinder. *IEEE Transactions on Antennas and Propagation* **66**, 3623–3630.
- Hyde MW, Bogle AE and Havrilla MJ (2013) Scattering of a partially-coherent wave from a material circular cylinder. *Optics Express* **21**, 32327–32339.
- Montaseri N, Abdolali A, Soleimani M and Nayyeri V (2012) Plane wave scattering by a circular PEMC cylinder coated with anisotropic media. *International Journal of RF and Microwave Computer-Aided Engineering* **23**, 225–231.
- Valenzuela-Sau JD, Munguia-Arvayo R, Gastelum-Acuna S, Gaspar-Armenta J, Napoles-Duarte J and Garcia-Llamas R (2017) Scattering of a Gaussian beam from a row of cylinders with rectangular cross section. *Journal of the Optical Society of America. A, Optics, Image Science, and Vision* **34**, 1369–1375.
- Zhang H, Huang Z and Shi Y (2013) Internal and near-surface electromagnetic fields for a uniaxial anisotropic cylinder illuminated with a Gaussian beam. *Optics Express* **21**, 15645–15653.
- Mao SC, Zhang ZH, Gao JS and Wu ZS (2019) Scattering of a Gaussian beam by an anisotropically coated circular cylinder. *Waves in Random and Complex Media* **29**, 54–62.
- Mao S-C, Wu Z-S, Zhang Z and Gao J (2017) Two-dimensional scattering of a Gaussian beam by a homogeneous gyrotropic circular cylinder. *International Journal of Microwave and Wireless Technologies* **9**, 1925–1929.
- Dikmen F, Sever E, Vatansver S and Tuchkin YA (2015) Well-conditioned algorithm for scattering by a few eccentrically multi-layered dielectric circular cylinders. *Radio Science* **50**, 99–110.
- Kriezis EE, Pandelakis PK and Papagiannakis AG (1994) Diffraction of a Gaussian beam from a periodic planar screen. *Journal of the Optical Society of America. A, Optics, Image Science, and Vision* **11**, 630–636.
- Valagiannopoulos CA and Tsitsas NL (2012) Field enhancement in a grounded dielectric slab by using a single superstrate layer. *Advances in OptoElectronics* **2012**, 1–9.
- Kozaki S (1982) A new expression for the scattering of a Gaussian beam by a conducting cylinder. *IEEE Transactions on Antennas & Propagation* **30**, 881–887.
- Ren W and Wu XB (1995) Application of an eigenfunction representation to the scattering of a plane wave by an anisotropically coated circular cylinder. *Journal of Physics D: Applied Physics* **28**, 1031–1039.
- Stratton JA (1941) *Electromagnetic Theory*. New York: McGraw-Hill.
- Beker B, Umashankar KR and Taflove A (1990) Electromagnetic scattering by arbitrarily shaped two-dimensions perfectly conducting objects coated with homogeneous anisotropic materials. *Electromagnetics* **10**, 387–406.



Shi-Chun Mao received his Ph.D. degree at Xidian University in 2010. His main research interests are electromagnetic and optical scattering.



Zhen-Sen Wu received his M.Sc. Degree at Wuhan University in 1981. He is currently a Professor at Xidian University. His research interests include electromagnetic and optical waves in random media, optical wave propagation and scattering, and ionospheric radio propagation.



Zhaohui Zhang received his M.Sc. degree at Jiangsu Normal University. He is good at MD simulations and QC simulations, the main programs used are Fortran, LAMMPS, VMD, Gaussian, and MS.



Jiansen Gao received his M.Sc. degree at Nanjing Normal University. His main research interest is Material physics.



Lijuan Yang received her M.Sc degree at Southeast University in 2006. Her main research interest is First-principles calculation of functional materials.